MEDWIN PUBLISHERS
Committed to Create Value for Researchers

International Journal of Pharmacognosy & Chinese Medicine
ISSN: 2576-4772

Synthesis of 3, 5-Disubstituted-Tetrahydro-2h-1, 3, 5-Thiadiazine-2-Thiones Derivatives and their Metal Complexes as Potential Bioactive Agents

Khan I[1]*, Ibrahim M[2], Shams F[1] and Ahmad MS[2]

[1]Institute of Chemical Sciences, University of Peshawar, Pakistan

[2]Department of Biosciences, Comsats University Islamabad, Pakistan

***Corresponding author:** Immad Khan, Institute of Chemical Sciences, University of Peshawar, Pakistan, Email: imadkhan358@uop.edu.pk

Research Article

Volume 7 Issue 2

Received Date: February 27, 2023

Published Date: July 12, 2023

DOI: 10.23880/ipcm-16000239

Abstract

Thiadiazine thione derivatives (2-(5-(2-.hydroxyethyl)-2-thioxo-1,3,5-thiadiazinane-3-yl) Acetic acid, 2-(5-.butyl-6-thioxo.-1, 3, 5-thiadiazinane-3-yl) Acetic acid, 2, 1 and 2 were synthesized by the reaction of alkyl primary amines (glycine, butylamine) with carbon disulfide and potassium hydroxide followed by addition of formaldehyde and various primary amines (ethanolamine, glycine) in phosphate buffer medium. The synthesized compounds were transformed into organometallic complexes (3-12) Ni (II), Co (II), Cu (II), Zn (II) and Fe (II) using their metal salts. The structure determinations of these compounds were elucidated by spectral methods such as IR, NMR spectroscopy and Mass spectrometry. All the synthesized compounds were screened for their anti-microbia++l activities. Their structure activity relationship showed that the potential of tested compounds enhanced with metal complexes against evaluated activities.

Keywords: Thiadiazine; Tetrahydrothiadiazine; Chloramphenicol; Nitroimidazoles

Introduction

Tetrahydro-2 H -l, 3, 5-thiadiazine-2-thione (THTT) derivatives are known to display important biological activities. Numerous studies have been published on their antibacterial1, antifungal11, anthelmintic17, antiprotozoal18, and antituberculous5 activity as prodrugs19. The antimicrobial activity of these compounds has been suggested to be based on isothiocyanates and dithiocarbamic acids, which are formed by hydrolysis of the tetrahydro-2H l, 3, 5-thiadiazine-2-thione ring 15-21. Some studies have pointed out the significance of the nature of the substituents at the 3- and 5-positions3-5. The study of the coordination behavior of thiones is of considerable interest due to their variable binding modes and because of the relevance of their binding sites to those in living systems [1-12].

The metal complexes of thiones have found great interest in recent research due to potent metal sulfur interaction which found several medicinal applications. These thiones are potentially ambidentate or multi-functional donors with either the exocyclic S or heterocyclic N atom available for coordination, thus yielding a variety of interesting complexes with geometries of variable nuclearities and great structural diversity [13]. Thiadiazine thione heterocyclic rings with various metal ions, have received much interest in biological applications. The recent reported DTTT gave unstable complexes in solution and were not isolated in solid form. The presence of oxygen moiety in metal complexes

can enhance antitumor activity of compounds. Similarly, antibacterial and antifungal activities of the complexes appear due to the chelating behavior of the ligands with most of the metal ions coordinated through N and S donor atoms. The novelty of present work to synthesized new THTT derivatives and transformed into their metal complexes to modify the thiadiazine thione nucleus [1].

Materials and Methods

General Procedure for the Synthesis of 3,5-Disubstiuted-Tetrahydrothiadiazine-2Thiones (P1-P4)

The glycine and butylamine (20 mmol) and potassium hydroxide (20%, 20 mmol) solution were stirred for 4 hour in 30 ml of water with drop wise addition of carbon disulphide (20 mmol). Followed by addition of 37% formaldehyde (40 mmol) stirred for 1h. The reaction mixture was filtered and was added drop-wise to a .suspension of ethanolamine and glycine in 20 ml of phosphate buffer solution (pH 7.8) with. Continued stirring for 1h. The aqueous solution was acidified with 15% HCl. The precipitate formed was filtered under suction and thoroughly. Washed with water. The product was recrystallized from ethanol. The reaction progress was monitored by TLC. Structure elucidation of the synthesized compounds were characterized by IR, 1H-NMR and elemental analysis.

Preparation of Complexes

Methanolic solution of metal salt (10 ml, 1 mmol) was added drop wise to a warm methanolic solution (10 ml) of THTT derivatives (1 mmol) for 2 h continuously stirred and refluxed in ambient temperature. A colored precipitate appeared was pass through filtered, washed with ethanol and was dried.

Preparation of Copper Complex [Cu (P1) So_4]$^{-2}$ (Cu1): Copper sulphate (0.16g, 1mmol) solution in methanol and was added.to magnetically stirred, warm methanol solution of ligand P1 (0.23g, 1mmol) and was further refluxed with stirring for 2hours. A green color precipitate appeared was pass through filtered, washed. with ethanol and was dried. Yield; 60%, m.pt. 281-283 oC, IR (KBr) cm-1: 690 (C=S), 514 (M-O), 612 (M-S), CHNS: cal; N,9.34; C,28.04; H,4.03; S,21.38, Found; N,8.74; C,27.40; H,3.53; S,22.00.

Preparation of Cobalt Complex [Co (P1) No_2]$^{-2}$ (Co1): Cobalt nitrate (0.18g, 1mmol) was dissolved in methanol and was added. to magnetically stirred and warm methanol solution of ligand P1 (0.23g, 1mmol) and was further refluxed with stirring for 2hours. A dark green color precipitate appeared was filtered, washed. with ethanol and dried. Yield; 75%, m.pt. 270-272°C, IR (KBr) cm^{-1}: 670 (C=S), 536 (M-O), 614 (M-S), CHNS: cal; N, 9.49; C, 28.48; H, 4.10; S, 21.72, Found; N, 5.50; C, 27.93; H, 4.41; S, 20.09.

Preparation of Zinc Complex [Zn (P1) CH_3COO]$^{-2}$ (Zn1): Zinc acetate (0.18g, 1mmol) was dissolved in methanol and was added.to magnetically stirred and warm methanol solution of ligand (0.23g, 1mmol) and was further refluxed with stirring for 2hours. A white color precipitate appeared was filtered, washed with ethanol and dried. Yield; 70%, m.pt.289-292°C, IR (KBr) cm^{-1}: 697 (C=S), 549 (M-O), 616 (M-S), CHNS: cal; C,27.87; H,4.03; N,9.29; S,21.38, Found; N,6.61; C,25.22; H,3.96; S,20.07.

Preparation of Nickel Complex [Ni (P1) So_4]$^{-2}$ (Ni1): Nickel sulphate (0.15g, 1mmol) was dissolved in methanol and was added.to magnetically stirred and warm methanol solution of ligand (0.23g, 1mmol) and was further refluxed with stirring for 2hours. A dark green color precipitate appeared was filtered, washed. With ethanol and dried. Yield; 75%, m.pt. 280-282°C, IR (KBr) cm^{-1}: 712 (C=S), 544 (M-O), 612 (M-S), CHNS: cal C,28.50; H,4.10; N,9.50; S,21.74, Found; C,27.93; H,4.24; N,8.66; S,16.74.

Preparation of Iron Complex [Fe (P1) Cl_2]$^{-2}$ (Fe1): Iron chloride (0.71g, 1mmol) was dissolved in methanol and was added. to magnetically stirred and warm methanol solution of ligand (0.23g, 1mmol) and was further refluxed with stirring for 2hours. A brown color precipitate appeared was filtered, washed. With ethanol and dried. Yield; 55%, m.pt. 232-234°C, IR (KBr) cm-1: 691 (C=S), 527 (M-O), 618 (M-S), CHNS: cal. C,28.78; H,4.14; N,9.59; S,21.95, Found: C,28.45; H,4.03; N,8.86; S,21.23.

Preparation of Copper Complex [Cu (P2) So_4]$^{-2}$ (Cu2): Copper sulphate (0.16g, 1mmol) was dissolved in methanol and was added. to magnetically stirred and warm methanol solution of P2 (0.24g, 1mmol) and was further refluxed with stirring for 2hours. A light green color precipitate appeared was filtered, washed. with ethanol and dried. Yield; 70%, m.pt. 271-273°C, IR (KBr) cm^{-1}: 702 (C=S), 612 (M-S), CHNS: cal; C,38.59; H,5.76; N,10.00; S,22.89, Found; C,31.41; H,5.80; N,11.86; S,21.52.

Preparation of Cobalt Complex [Co (P2) No_2]$^{-2}$ (Co2): Cobalt nitrate (0.18g, 1mmol) was dissolved in methanol and was added. to magnetically stirred and warm methanol solution of P2 (0.24g, 1mmol) and was further refluxed with stirring for 2hours. A green color precipitate appeared was filtered, washed with ethanol and dried. Yield; 70%, m.pt. 279-281°C, IR (KBr) cm^{-1}: 701 (C=S), 611 (M-S), CHNS: cal. C,37.56; H,5.85; N,9.59; S,22.92, Found: C,35.59; H,5.19; N,7.74; S,25.22.

Preparation of Zinc Complexes [Zn (P2) CH_3COO]$^{-2}$ (Zn2):

Zinc acetate (0.18g, 1mmol) was dissolved in methanol and was added. to magnetically stirred and warm methanol solution of ligand (0.24g, 1mmol) and was further refluxed with stirring for 2hours. A white color precipitate appeared was filtered, washed with ethanol and dried. Yield; 75%, m.pt. 299-302°C, IR (KBr) cm^{-1}: 710 (C=S), 597 (M-S), CHNS: cal; C,31.20; H,4.66; N,8.09; S,28.31 Found; C,36.16; H,5.76; N,8.42; S,25.87.

Preparation of Nickel Complex [Ni (P2) So_4]$^{-2}$ (Ni2): Nickel sulphate (0.24g, 1mmol) was dissolved in methanol and was added. to magnetically stirred and warm methanol solution of ligand (0.24g, 1mmol) and was further refluxed with stirring for 2hours. A dark green color precipitate appeared was filtered, washed. with ethanol and dried. Yield; 70%, m.pt. °C, IR (KBr) cm^{-1}: 698 (C=S), 612 (M-S), CHNS: cal. C,32.13; H,4.79; N,8.33; S,19.06, Found; C,32.74; H,5.42; N,7.34; S,16.00.

Preparation of Iron Complexes [Fe (P2) Cl_2]$^{-2}$ (Fe_2): Iron chloride (0.71g, 1mmol) was dissolved in methanol and was added. to magnetically stirred and warm methanol solution of ligand (0.24g, 1mmol) and was further refluxed with stirring for 2hours. A reddish brown color precipitate appeared was filtered, washed. with ethanol and dried. Yield; 60%, m.pt. 241-243°C, IR (KBr) cm^{-1}: 701 (C=S), 597 (M-S), CHNS: cal. C,39.13; H,5.84; N,10.14; S,23.21, Found; C,38.74; H,5.56; N,9.34; S,23.12.

Results and Discussion

According to the propose work attempt to synthesized a series of thiadiazine thione derivatives transformed into their organometallic complexes. The purification of the products were determined by TLC and melting point.

5-(2-Hydroxyethyl)-2-Thioxo-1, 3, 5-Thiadiazinan-3-Yl] Acetic Acid (1)

^{1}H-Nmr (400 Mhz, Cd3od) Data of [5-(2-Hydroxyethyl)-2-Thioxo-1, 3, 5-Thiadiazinan-3-Yl] Acetic Acid (1) Table 1.

δ (ppm)	Assignment	Multiplicity	Integration	*J* (Hz)
4.79	C-4	s	2H	---
4.75	C-6	s	2H	---
4.56	C-7	s	2H	---
3.72	C-9	t	2H	5.4
3.07	C-10	t	2H	5.4

Table 1: ^{1}H-Nmr5 (400 MHz, Cd3od) Data of [5-(2-Hydroxyethyl)-2-Thioxo-1, 3, 5- Thiadiazinan-3-Yl] Acetic Acid (1).

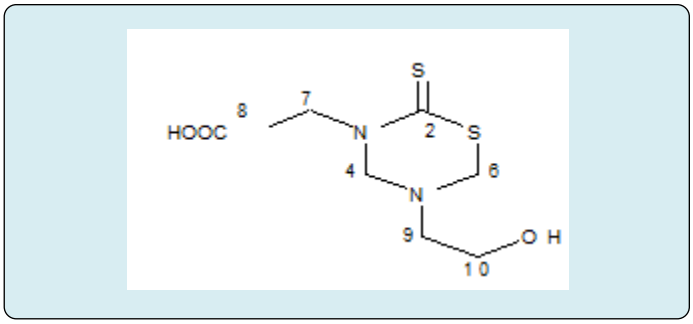

[5-(2-Hydroxyethyl)-2-Thioxo-1, 3, 5-Thiadiazinan-3-Yl] Acetic Acid (1)

In the ^{1}H-NMR of (1), the two singlet's at δ 4.79 and δ 4.75 were due to protons at C-4 and C-6 respectively: the distinguishing peaks of the THTT nucleus. Similarly, the singlet at δ 4.56 was due to protons of C-7. The two triplets at δ 3.72 and δ 3.07 were due to protons of C-9 and C-10. 1H-NMR characterized the proposed structure of [1].

2-(5-Butyl-6-Thioxo-1, 3, 5- Thiadiazinan-3-Yl) Acetic Acid (2)

δ (ppm)	Assignment	Multiplicity	Integration	*J* (Hz)
4.53	C-4	S	2H	---
4.52	C-6	S	2H	---
3.97	C-7	T	2H	7.8
3.30	C-11	S	2H	---
1.671.61	C-8	M	2H	---
1.38-1.33	C-9	M	2H	---
0.96	C-10	T	3H	7.3

Table 2: ^{3}C-NMR (75 MH z, CD3OD) Data of (5-BUTYL-6-THIOXO-1, 3, 5-THIADIAZINAN 3-Yl) Acetic Acid (2).

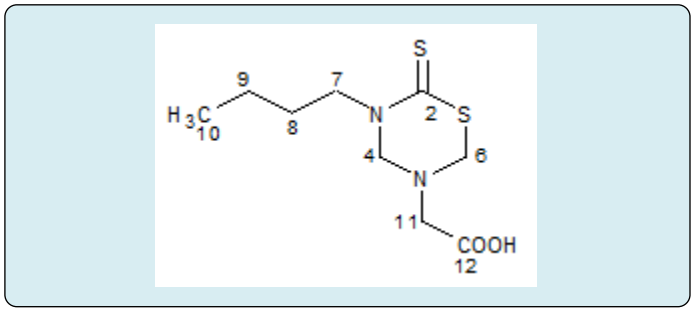

2-(5-BUTYL-6-THIOXO-1, 3, 5-THIADIAZINAN-3YL) Acetic Acid (2)

^{1}H-NMR (500 MHz, CD3OD) data of (5-butyl-6-thioxo-1, 3, 5-thiadiazinan-3-yl) acetic acid (2) Table 3.

δ (ppm)	Assignment	Multiplicity	Integration	*J* (Hz)
4.53	C-4	S	2H	---
4.52	C-6	S	2H	---
3.97	C-7	T	2H	7.8
3.3	C-11	S	2H	---
1.671.61	C-8	M	2H	---
1.38-1.33	C-9	M	2H	---
0.96	C-10	T	3H	7.3

Table 3: ^{3}C-NMR (75 MHZ, CD3OD) Data of (5-BUTYL-6-THIOXO-1, 3, 5-THIADIAZINAN 3-YL) Acetic Acid (2).

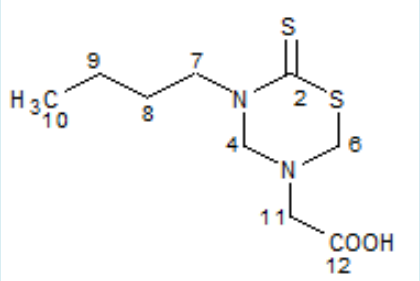

2-(5-BUTYL-6-THIOXO-1, 3, 5-THIADIAZINAN-3YL) ACETIC ACID (2)

In ^{1}H-NMR spectrum of the compound [2], the two singlets at δ 4.53, δ 4.52 were assigned to protons at C-4 and C-6, respectively, which are the typical peaks of THTT nucleus. Similarly, the triplets at δ 3.97 and δ 0.96 were due to protons at C-7 and C-10. The multiplets at δ 1.67-1.61 and δ 1.38-1.30 were assigned to protons at C-8 and C-9 positions due to non-equivalent protons in the environment (Table 4).

Assign ment	δ (ppm)	Assign ment	δ (ppm)	Assign ment	δ (ppm)
C-2	192.8	C-6	59.4	C-9	20.9
C-12	172.8	C-7	52.0	C-10	14.1
C-4	70.9	C-8	29.5		

Table 4: Protons at C-8 and C-9 positions due to non-equivalent protons in the environment.

In ^{13}C-NMR spectrum of the compound (2), the signals at δ 192.8, δ 70.9 and δ 59.4 were due to C-2, C-4 and C-6, respectively which are the typical peaks of THTT nucleus. The signal at δ 172.8 is the prominent peak of the carboxylic carbon (C-12). The signals at δ δ 52.0, δ 29.5, δ 20.9 and δ 52.9 were assigned to methylenic carbons, C-7, C-8, C-9 and C-11. The most upfield signal at δ 14.1 was assigned to methyl carbon (C-10).

Mass spectrum of (2), showed molecular ion (M+) at m/z 248 while other peaks with their relative intensities are m/z 115 (22), 84 (86), 72 (96), 60 (58) and 57 (100). Anal. Calcd for $C_9H_{16}N_2O_2S_2$: C, 43.54; H, 6.45; N, 11.29. Found: C, 43.06; H, 6.53; N, 11.04. The spectral data obtained from NMR, MS and elemental analysis characterized the proposed structure of [2].

Structure Elucidation of Metal Complexes

Complex/ Ligand	C=S	C-OH	Aliphatic C-H	M-O	M-S
1(ligand)	1435 cm^{-1}	3310 cm^{-1}	2850 cm^{-1}	-	-
$[Cu(1)SO4]^{-2}$	690 cm^{-1}			514 cm^{-1}	612 cm^{-1}

Table 5: R (KBr υ max cm^{-1}) data of Copper metal complex $[Cu\ (1)\ SO_4]^{-2}$ (3).

Sample code	%N	%C	%H	%S
-5	8.74	27.40	3.53	22.00

Table 6: CHNS analysis of complex [3].

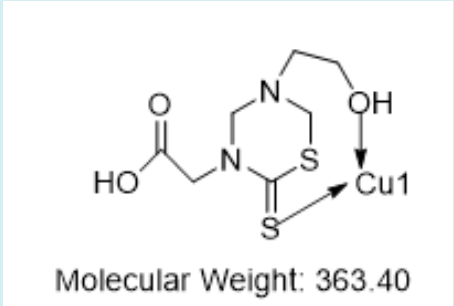

Structure of (3)

IR data of compound 1 and their Copper metal complex showed peaks in which C=S band of 1 (ligand) appear in 1435 cm^{-1} and their metal complex C=S peak absorbed in 690 cm^{-1}. While the M-S band absorbed in 612 cm^{-1} indicate that 1 involved to copper metal for their complexation. Similarly the enolic band of 1 absorbed at 3310 cm^{-1} and M-O region 514 cm^{-1} indicate the metal and hydroxyl involvement. CHNS analysis found for $[Cu\ (1)\ SO_4]$; N: 8.74; C: 27.40; H: 3.53; S: 22.00. The obtained data confirm the propose structure of $[Cu\ (1)\ SO_4]^{-2}$ (3) Table 7 and Table 8.

Complex/ Ligand	C=S	C-OH	Aliphatic C-H	M-O	M-S
1(ligand)	1435 cm^{-1}	3310 cm^{-1}	2850 cm^{-1}	-	-
$[Co(1)NO_2]^{-2}$	670 cm^{-1}			536 cm^{-1}	614 cm^{-1}

Table 7: IR (KBr υ max cm^{-1}) data of Cobalt metal complex $[Co\ (1)\ NO_2]^{-2}$ [4].

Sample code	%N	%C	%H	%S
(6)	5.50	27.93	4.41	20.09

Table 8: CHNS analysis of complex [4].

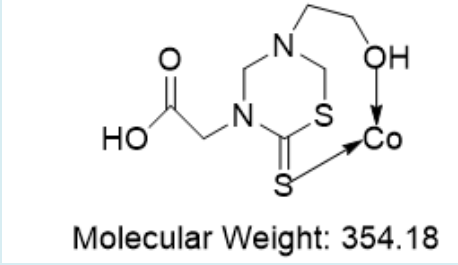

Structure of (4)

IR data of compound 1 and their Cobalt metal complex showed peaks in which C=S band of 1 (ligand) appear in 1435 cm^{-1} and their metal complex C=S peak absorbed in 670 cm^{-1}. While the M-S band absorbed in 614 cm^{-1} indicate that 1 involved to cobalt metal for their complexation. Similarly the enolic band of 1 absorbed at 3310 cm-1 and M-O region 536 cm^{-1} indicate the metal and hydroxyl involvement. CHNS analysis found for [Co (1) NO2]; N: 5.50; C: 27.93; H: 4.41; S: 20.09. The obtained data confirm the propose structure of $[Co\ (1)\ NO_2]^{-2}$ (4) Table 9 and Table 10.

Complex/ Ligand	C=S	C-OH	Aliphatic C-H	M-O	M-S
1(ligand)	1435 cm^{-1}	3310 cm^{-1}	2850 cm^{-1}	-	-
[Zn(1) CH_3COO]	697 cm^{-1}			549 cm^{-1}	616 cm^{-1}

Table 9: IR (KBr υ max cm-1) data of Zinc metal complex $[Zn\ (1)\ CH_3COO]^{-2}$ (5).

Sample code	%N	%C	%H	%S
(7)	6.61	25.22	3.96	20.07

Table 10: CHNS analysis of complex [5].

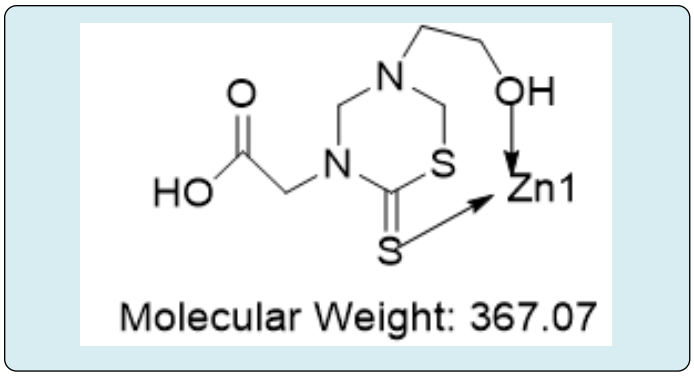

Structure of (5)

IR data of compound 1 and their Zinc metal complex showed peaks in which C=S band of 1 (ligand) appear in 1435 cm^{-1} and their metal complex C=S peak absorbed in 697 cm^{-1}. While the M-S band absorbed in 616 cm^{-1} indicate that 1 involved to copper metal for their complexation.

Similarly the enolic band of 1 absorbed at 3310 cm^{-1} and M-O region 549 cm^{-1} indicate the metal and hydroxyl involvement. CHNS analysis found for [Zn (1) CH_3COH]; N: 6.61; C: 25.22; H: 3.96; S: 20.07. The obtained data confirm the propose structure of $[Zn\ (1)\ CH_3COO]^{-2}$ (5) Table 11 and Table 12.

Complex/ Ligand	C=S	C-OH	Aliphatic C-H	M-O	M-S
1(ligand)	1435 cm^{-1}	3310 cm^{-1}	2850 cm^{-1}	-	-
$[Ni(1)SO_4]^{-2}$	712 cm^{-1}			544 cm^{-1}	612 cm^{-1}

Table 11: IR (KBr υ max cm-1) data of Nickel metal complex $[Ni\ (2)\ SO_4]^{-2}$ (6).

Sample code	%N	%C	%H	%S
(8)	8.66	27.93	4.24	16.74

Table 12: CHNS analysis of complex [6].

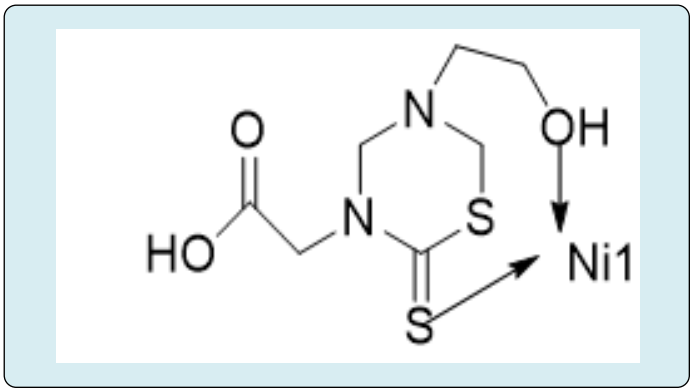

Structure of (6)

IR data of compound 1 and their Nickel metal complex showed peaks in which C=S band of 1 (ligand) appear in 1435 cm^{-1} and their metal complex C=S peak absorbed in 712 cm^{-1}. While the M-S band absorbed in 612 cm^{-1} indicate that 1 involved to copper metal for their complexation. Similarly the enolic band of 1 absorbed at 3310 cm^{-1} and M-O region 544 cm^{-1} indicate the metal and hydroxyl involvement. CHNS analysis found for [Ni (P1) SO_4]; N: 8.66; C: 27.93; H: 4.24; S: 16.74. The obtained data confirm the propose structure of [Ni (1) SO_4]$^{-2}$ (6) Table 13 and Table 14.

Complex/ Ligand	C=S	C-OH	Aliphatic C-H	M-O	M-S
1(ligand)	1435 cm-1	3310 cm^{-1}	2850 cm^{-1}	-	-
[Fe(1)Cl_2]$^{-2}$	691 cm^{-1}			527 cm^{-1}	618 cm^{-1}

Table 13: IR (KBr υ max cm^{-1}) data of Copper metal complex [Fe (1) Cl_2]$^{-2}$ (7).

Sample code	%N	%C	%H	%S
(9)	8.86	28.45	4.03	21.23

Table 14: CHNS analysis of complex [7].

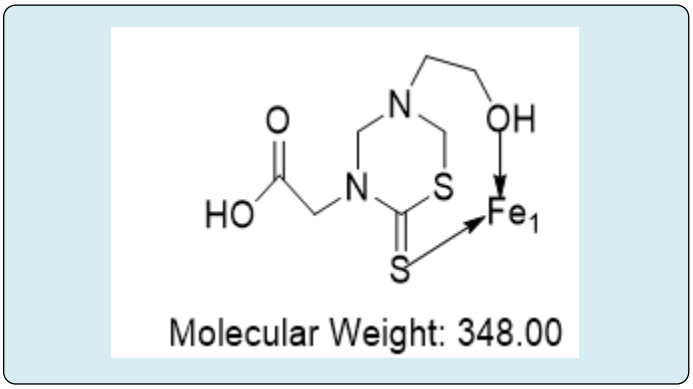

Structure of (7)

IR data of compound 1 and their Iron metal complex showed peaks in which C=S band of 1 (ligand) appear in 1435 cm^{-1} and their metal complex C=S peak absorbed in 691 cm^{-1}. While the M-S band absorbed in 618 cm^{-1} indicate that 1 involved to copper metal for their complexation. Similarly the enolic band of 1 absorbed at 3310 cm^{-1} and M-O region 527 cm^{-1} indicate the metal and hydroxyl involvement. CHNS analysis found for [Fe (1) Cl]; N: 8.86; C: 28.45; H: 4.03; S: 21.23. The obtained data confirm the propose structure of [7] Table 15 and Table 16.

Complex/ Ligand	C=S	COOH	Aliphatic C-H	M-S
2(ligand)	1488 cm^{-1}	3420 cm^{-1}	2954 cm^{-1}	-
[Cu(2)SO4]$^{-2}$	702 cm^{-1}			612 cm^{-1}

Table 15: IR (KBr υ max cm^{-1}) data of Copper metal complex [Cu (2) SO_4]$^{-2}$ (8).

Sample code	%N	%C	%H	%S
(10)	11.86	36.41	5.80	21.52

Table 16: CHNS analysis of complex [8].

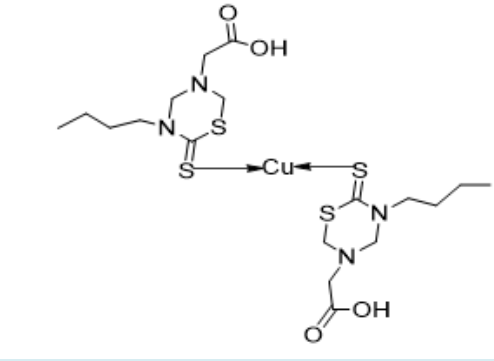

Structure of (8)

IR data of compound 2 and their Copper metal complex showed peaks in which C=S band of 2 (ligand) appear in 1488 cm^{-1} and their metal complex C=S peak absorbed in 702 cm^{-1}. While the M-S band absorbed in 612 cm^{-1} indicate that 2 involved to copper metal for their complexation. CHNS analysis found for [Cu (2) SO_4]; N: 11.86; C: 36.41; H: 5.80; S: 21.52. The obtained data confirm the propose structure of [Cu (2) SO_4] (8) Table 17 and Table 18.

Sample code	%N	%C	%H	%S
(11)	7.74	35.59	5.19	25.22

Table 17: IR (KBr υ max cm^{-1}) data of Cobalt metal complex [Co (2) NO_2]$^{-2}$ (9).

Complex/ Ligand	C=S	C-OH	Aliphatic C-H	M-S
2(ligand)	1488 cm^{-1}	3420 cm^{-1}	2954 cm^{-1}	-
[Co(2)NO_2]$^{-2}$	701 cm^{-1}			611 cm^{-1}

Table 18: CHNS analysis of complex [9].

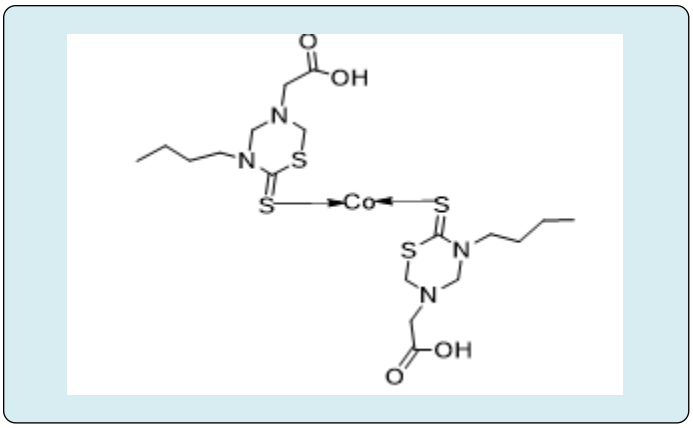

Structure of (9)

IR data of compound 2 and their Cobalt metal complex showed peaks in which C=S band of 2 (ligand) appear in 1488 cm^{-1} and their metal complex C=S peak absorbed in 701 cm^{-1}. While the M-S band absorbed in 611 cm^{-1} indicate that 2 involved to Cobalt metal for their complexation. CHNS analysis found for [Co (2) NO_2]; N: 7.74; C: 35.19; H: 5.19; S: 25.22. The obtained data confirm the propose structure of [Co (P2) NO_2]$^{-2}$ (9) Table 19 and Table 20.

Complex/ Ligand	C=S	C-OH	Aliphatic C-H	M-S
2(ligand)	1488 cm^{-1}	3420 cm^{-1}	2954 cm^{-1}	-
[Zn (P2) CH_3COO]	710 cm^{-1}			597 cm^{-1}

Table 19: IR (KBr υ max cm^{-1}) data of Zinc metal complex [Zn (2) CH_3 COO]$^{-2}$ (10).

Sample code	%N	%C	%H	%S
(12)	8.42	36.16	5.76	25.87

Table 20: CHNS analysis of complex [10].

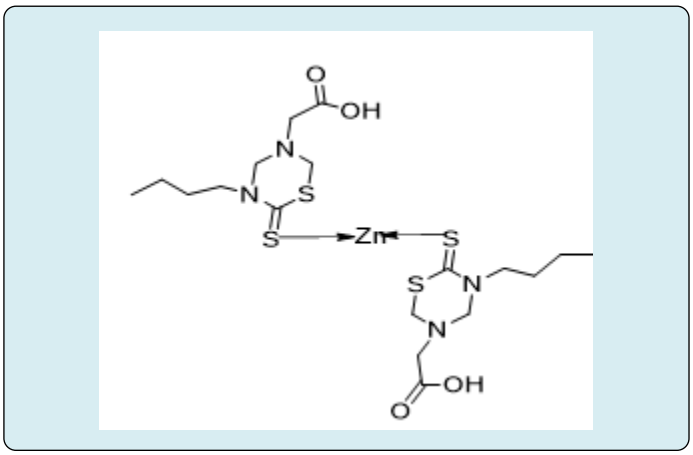

Structure of (10)

IR data of compound 2 and their Zinc metal complex showed peaks in which C=S band of 2 (ligand) appear in 1488 cm^{-1} and their metal complex C=S peak absorbed in 710 cm^{-1}. While the M-S band absorbed in 597 cm^{-1} indicate that 2 involved to Zinc metal for their complexation. CHNS analysis found for [Zn (P2) SO4]; N: 8.42; C: 36.16; H: 5.76; S: 25.87. The obtained data confirm the propose structure of [Zn (2) CH_3 COO]$^{-2}$ (10) Table 21 and Table 22.

Complex/ Ligand	C=S	C-OH	Aliphatic C-H	M-S
2(ligand)	1488 cm^{-1}	3420 cm^{-1}	2954 cm^{-1}	-
[Ni(2)SO4]$^{-2}$	698 cm^{-1}			612 cm^{-1}

Table 21: IR (KBr υ max cm^{-1}) data of Nickel metal complex [Ni (2) SO_4]$^{-2}$ (11)

Sample code	%N	%C	%H	%S
(13)	7.34	32.74	5.42	16.00

Table 22: CHNS analysis of complex [11].

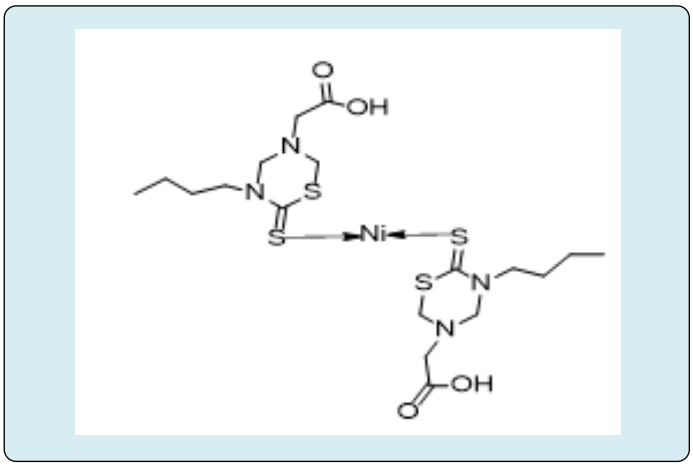

Structure of (11)

IR data of compound 2 and their Nickel metal complex showed peaks in which C=S band of 2 (ligand) appear in 1488 cm^{-1} and their metal complex C=S peak absorbed in 698 cm^{-1}. While the M-S band absorbed in 612 cm^{-1} indicate that 2 involved to Nickel metal for their complexation. CHNS analysis found for [Ni (P2) SO_4]; N: 7.34; C: 32.74; H: 5.42; S: 16.00. The obtained data confirm the propose structure of [Ni (2) SO_4]$^{-2}$ (11).

Complex/ Ligand	C=S	C-OH	Aliphatic C-H	M-S
2(ligand)	1488 cm^{-1}	3420 cm^{-1}	2954 cm^{-1}	-
$[Fe(2)Cl_2]^{-2}$	701 cm^{-1}			597 cm^{-1}

Table 23: IR (KBr υ max cm^{-1}) data of Iron metal complex [Fe (2) $Cl_2]^{-2}$ (12).

Sample code	%N	%C	%H	%S
(14)	9.34	38.74	5.56	23.12

Table 24: CHNS analysis of complex [12].

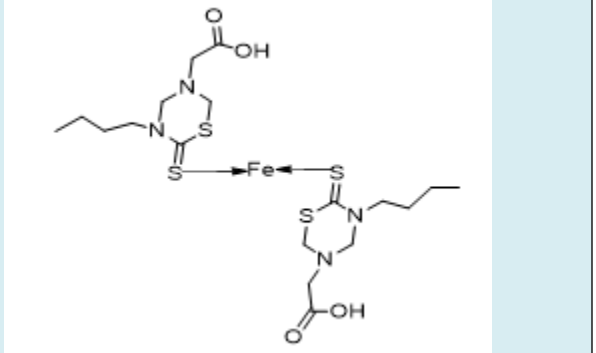

Structure of (12)

IR data of compound 2 and their iron metal complex showed peaks in which C=S band of 2 (ligand) appear in 1488 cm^{-1} and their metal complex C=S peak absorbed in 701 cm^{-1}. While the M-S band absorbed in 597 cm^{-1} indicate that 2 involved to Iron metal for their complexation.

CHNS analysis found for [Fe (1) Cl_2]; N: 9.34; C: 38.74; H: 5.56; S: 23.12. The obtained data confirm the propose structure of [Fe (2) $Cl_2]^{-2}$ (12).

Biological Evaluation of Antimicrobial Studies

The wide spread research and studies in the field of antimicrobial drugs has played a pivotal role for the development and synthesis of a large number of drugs including penicillin, aminoglycosides, carbenems, tetracyclines, streptogramins, monobactam, cephalosporins, miconazole and macrolides38. The cure of .numerous disease is done by these great numbers of drugs. But now unfortunately the situation has changed totally due to the increase in the number of immuno-compromised hosts 39 and it is evident from the number of reports that bacterial population showed .sever resistance to majority of antibacterial agents such as ß-lactam antibiotics, sulfonamide drugs, and nitroimidazoles (DNA inhibitors), macrolides and chloramphenicol [13].

From some other reports the resistance to antifungal agents such as azoles in candida species, and also their failure in the treatment of fungal infections has been evidenced41 and the majority of the antifungal drugs are silent against invasive aspergilliosis and now amphotericin. B is the only drug used in such patients. Also some better antifungal agents are strongly required for diseases like systemic .mycosis and neoplasia. These facts and figures make researchers to develop some new highly active broad spectrum drug agents [14-22].

Thus keeping in view the above mentioned background, the synthesized compounds were screened with the expectation that they might have an aggressive activity against such resistant microbes as compared to the drugs available in the market.

Antimicrobial Bioassay (*In vitro*)

The synthesized compounds were screened *in vitro* for their antibacterial activities against Xanthomonas campestris and Erwinia cartovora bacterial strains using literature protocol of to determine the antibacterial activity. The Nutrient Broth. (Oxide, UK) media was prepared of 3.25g in 100ml of distilled water in Autoclavable conical flask. The media were dissolved through Thermo. Magnetic stirrer and put it in the Autoclave at 121 ºC of 15 lbs for 15 minutes due to sterilization of media. The media were prepared for bacterial growth and were used as stock.bacteria growth. The available nutrient agar media were dissolved of about 2.8 g in 100ml of distilled water by the help of magnetic stirrer in 250ml autoclavable bottle. After the dissolution media was lefted for 15 minutes in Autoclave for sterilization at 121 ºC of 15 lbs. Autoclaved media was safely transferred to laminar hood. Media was poured in sterilized petri dishes (20ml media per petri dish) and left it for 15minutes for coldness. When the media become cold and appear like a jelly. The sterile cotton swab was stitched on the nutrient agar medium surface for the inoculation of microbes and then make wells on the plates.

The extract was present in Serum cups that shake welled before use on vertex mixer applied with the concentration of 3µl, 6µl and 9µl per well with the help of micropipette. The plates were kept for one hour in refrigerator at -20 ºC and then transferred to incubator at 37 ºC for 24 hours. Ciprofloxacin which is wide range spectrum antibiotic were used as positive control with concentration of 50µg/6µl for

both gram positive and gram negative bacteria strain. DMSO was used as negative control for bacterial and fungal strain.

Xanthomonas Campestris				Erwinia Cartovora		
Sample	**3µg**	**6µg**	**9µg**	**3µg**	**6µg**	**9µg**
Fe_2 (14)	21	21	22.3	15	18	19.6
Cu_2 (10)	15.6	18	21	19	19	21
P_2 (2)	19	20	21	20	20.6	21
Fe_1 (9)	16	19	19	17	18	19.6
Zn_2 (12)	24	21	22	16	19	21
P_1 (1)	17	20	20.6	16	20	19.3
Ni_1 (8)	21	22.3	22	18	17.6	20.6
Co_1 (6)	17	18.6	20.6	21	21.6	22
Zn_1 (7)	23	22	23	18	19.6	20.6
Ni_2 (13)	21	24	23.6	15	18	18.3
Cu_1 (5)	23	22	23	20	19	21
Control	28	31	35	28	29	31

Table 25: Cu_1 of complex (3), Cu_2 of complex (8), Ni1 of complex (6), Ni2 of complex (11), Co_1 of complex (4), Co_2 of complex (9), Zn_1 of complex (5), Zn_2 of complex (10), Fe1 of complex (7), Fe_2 of complex (12).

Result of Antibacterial Activity

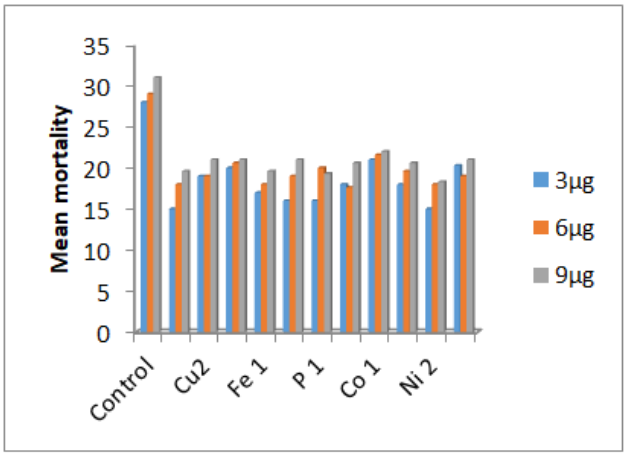

Figure 1: Graph for Xanthomonas Campestris (mean mortality).

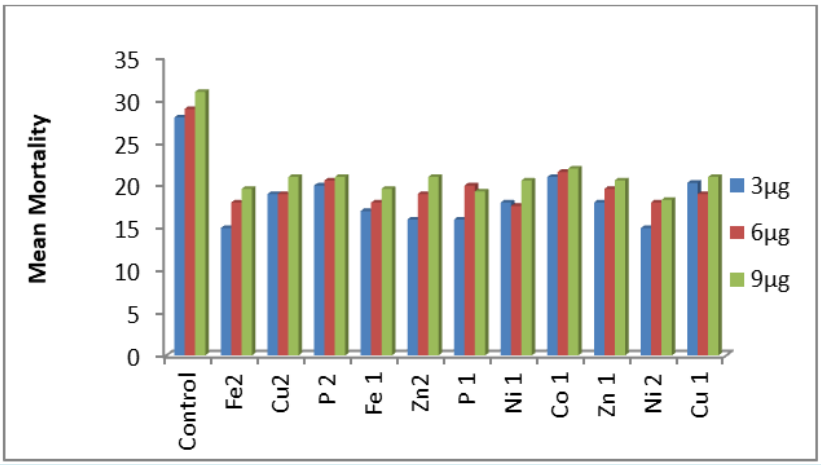

Figure 2: Graph For Erwinia Cartovora (mean mortality).

Discussion

Against Xanthomonas campestris, the mortality showed in 3µg that the highest mortality (24) caused by (10), the highest (24) mortality was caused by (11) in 6µg, while the highest (23.6) was caused by (11) in 9 µg. The (1), (2), (4), (8), observed most effective was found concentration depended increased by increasing of concentration. Among all compounds the highest mortality (24) was caused by (10) and (11) and was observed maximum as increasing the concentrations.

Against Erwinia cartovora, the mortality showed that the highest mortality (21) was cause by (4) in 3µg and the highest (21.6) mortality was caused by (4) in 6µg, while the highest (22) was caused by (4) in 9 µg. The (5), (7), (10), (12), observed most effective was found concentration depended increased by increasing of concentration. Among all compounds the highest mortality (22) was caused by (4) and was observed maximum as increasing the concentrations as showed in Table.

Antifungal Bioassay (*In vitro*)

The synthesized compounds were used against Rhizopus stolonifer, Rhizocotina solani, *in vitro* for their antifungal activities. Nutrient Broth (Oxide, UK) media was prepared of 3.25g in 100ml of distilled water in Autoclavable conical flask. The media were dissolved through Thermo Magnetic stirrer and put it in the Autoclave at 121 ºC of 15 lbs for 15minutes due to sterilization of media. The media were prepared for bacterial growth and were used as stock bacteria growth. The Potato Dextrose Agar media was prepared of 0.039g in 100ml of distilled water in Autoclavable bottle. Media was dissolved through Thermo Magnetic stirrer and put it in the .Autoclave at 121 ºC of 15 lbs for 15minutes due to sterilization of media. The media was prepared for fungal growth. Autoclaved media was safely transferred to laminar hood. Media was poured in sterilized petri dishes (20ml media per petri dish) and left it for 15 minutes for coldness.

When the media become cold and seemed to be jelly like. The sterile cotton swab was stitched on the nutrient agar medium surface for the inoculation of microbes and then make wells on the plates. The extract was present in Serum cups that shake welled before use on vertex mixer applied with the concentration of 3µl, 6µl and 9µl per well with the help of micropipette. The plates were kept for one h in refrigerator at -20 ºC and then transferred to incubator at 37 ºC for 24 hours. Nystatine was used as positive control for fungi. DMSO was used as negative control for bacterial and fungal strain.

Results of Antifungal Activity

Rhizopus stolonifer				Rhizocotina solani		
Sample	**3µg**	**6µg**	**9µg**	**3µg**	**6µg**	**9µg**
Fe_2 (14)	20	20	21.3	16	17	17.6
Cu_2 (10)	16	18.6	20	18	18	20.3
P_2 (2)	18.3	19.6	20	19.6	20	20
Fe_1 (9)	17	19.3	19.5	17	18	19.6
Zn_2 (12)	22.3	24	24.5	18	19.3	21.5
P_1 (1)	18	20	20.6	17	20	19.3
Ni_1 (8)	20	22.3	22.7	18	19.6	21.6
Co_1 (6)	17	18.6	20.6	21	21.6	22
Zn_1 (7)	23	24	25	19	20.6	22.6
Ni_2 (13)	21.3	24	23.6	17	19	19.8
Cu_1 (5)	23	22	23	20.3	19	21
Control	28	31	35	28	29	31

Table 26: Cu_1 of complex (3), Cu_2 of complex (8), Ni_1 of complex (6), Ni_2 of complex (11), Co_1 of complex (4), Co_2 of complex (9), Zn_1 of complex (5), Zn_2 of complex (10), Fe_1 of complex (7), Fe_2 of complex (12).

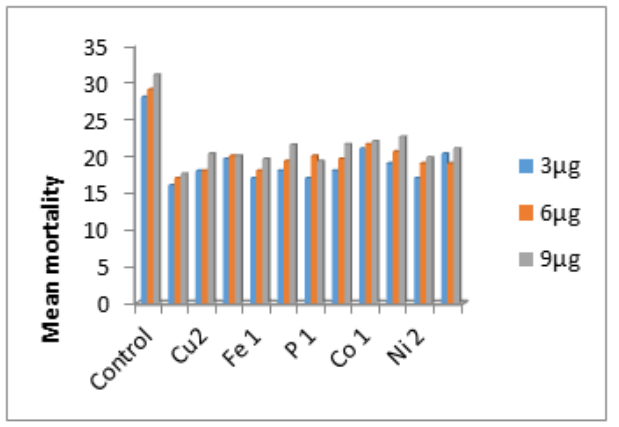

Figure 3: Graph for *Rhizopus stolonifer* (mean mortality).

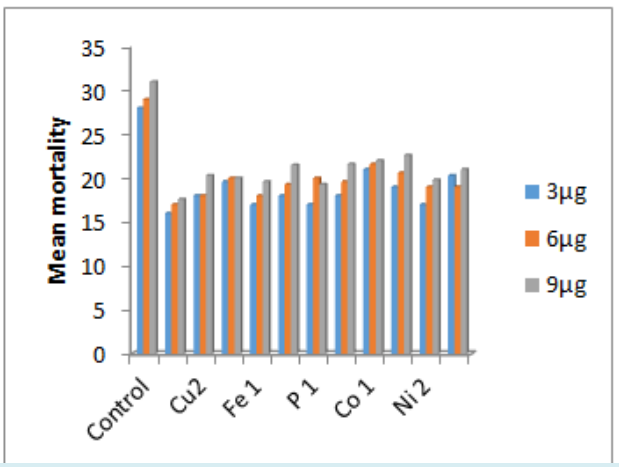

Figure 4: Graph for *Rhizocotina solani* (mean mortality).

Against Rhizopus stolonifer, the mortality showed in 3µg that the highest mortality (23) caused by (3), the highest (24) mortality was caused by (10) and (11) in 6µg, while the highest (25) was caused by (5) in 9 µg. The (1), (2), (4), (7), (8) observed most effective was found concentration depended increased by increasing of concentration. Among all compounds the highest mortality (25) was caused by (5) and was observed maximum as increasing the concentrations.

Against Rhizocotina solani the mortality showed that the highest mortality (21) was cause by (4) in 3µg and the highest (21.6) mortality was caused by (4) in 6µg, while the highest (22) was caused by (4) in 9 µg. The (5), (8), (10), (12) observed most effective was found concentration depended increased by increasing of concentration. Among all compounds the highest mortality (22) was caused by (4) and was observed maximum as increasing the concentrations as showed in Table.

Author Contributions

All the authors have accepted responsibility for the entire content of this submitted manuscript and have approved its submission.

Conflict of Interest

This study has no conflict of interest to be declared by any author.

Funding

The author(s) received no financial support for the research, authorship, and/or publication of this article.

Acknowledgement

We would like to special thanks to Pakistan Council of Scientific and Industrial Research, administrator, data collector and study participants.

References

1. Neochoritis C, Tsoleridis CA, Stephanidou Stephanatou J (2008) 1-Arylaminoimidazole-2-thiones as intermediates in the synthesis of imidazo 2, 1-b 1, 3, 4 thiadiazines. Tetrahedron 64(16): 3527-3533.

2. Erdem SS, Özpınar GA, Saçan MT (2005) Investigation on the aromaticity of 1, 3, 4-thiadiazole-2-thione and its oxygen analogs including their tautomeric forms. Journal of Molecular Structure Theochem 726(1-3): 233-243.

3. Zhu F, Fan W, Wang A, Zhu Y (2009) Tribological study of novel S N style 1, 3, 4 thiadiazole-2-thione derivatives in rapeseed oil. Wear 266(1-2): 233-238.

4. Weisburger JH (2002) Comments on the history and importance of aromatic and heterocyclic amines in public health. Mutation Research Fundamental and Molecular Mechanisms of Mutagenesis 506: 9-20.

5. Singh AK, Mishra G, Jyoti K (2011) Review on biological activities of 1, 3, 4-thiadiazole derivatives. Journal of applied pharmaceutical science 1(5): 44-49.

6. Bermello JC, Piñeiro RP, Fidalgo LM, Cabrera HR, Navarro MS (2011) Thiadiazine derivatives as antiprotozoal new drugs. The Open Medicinal Chemistry Journal 5: 51-60.

7. Aboul Fadl T, Hussein MA, Shorbagi EI, Khallil AR (2002) New 2H-Tetrahydro-1, 3, 5-thiadiazine-2-thiones Incorporating Glycine and Glycinamide as Potential Antifungal Agents. Archiv der Pharmazie 335(9): 438-442.

8. Rodríguez H, Suárez M, Albericio F (2012) Thiadiazines NN-heterocycles of biological relevance. Molecules 17(7): 7612-7628.

9. Echemendía R, Fernández O, Coro J, Suárez M, Rivera DG (2017) A versatile approach to hybrid thiadiazine-based molecules by the Ugi four-component reaction. Tetrahedron letters 58(18): 1784-1787.

10. Hemantha HP, Sureshbabu VV (2009) A simple approach for the synthesis of new classes of dithiocarbamate linked peptidomimetics. Tetrahedron Letters 50(50): 7062-7066.

11. Coro J, Atherton R, Little S, Wharton H, Yardley V, et al. (2006) Alkyl linked bis THTT derivatives as potent in vitro trypanocidal agents. Bioorganic medicinal chemistry letters 16(5): 1312-1315.

12. Radwan AA, Al-Dhfyan A, Abdel Hamid MK, Al Badr AA, Aboul Fadl T (2012) 3, 5-Disubstituted thiadiazine-2-thiones New cell-cycle inhibitors. Archives of pharmacal research 35(1): 35-49.

13. Coro J, Atherton R, Little S, Wharton H, Yardley V, et al. (2006) Alkyl-linked bis THTT derivatives as potent in vitro trypanocidal agents. Bioorganic medicinal chemistry letters 16(5): 1312-1315.

14. Amin RM, Abdel Kader NS, El Ansary AL (2012) Microplate assay for screening the antibacterial activity of Schiff bases derived from substituted benzopyran-4-one. Spectrochimica Acta Part A Molecular and Biomolecular Spectroscopy 95: 517-525.

15. Rodríguez H, Suárez M, Albericio F (2012) Thiadiazines N, N-heterocycles of biological relevance. Molecules 17(7): 7612-7628.

16. Ochao C, Perez E, Perez R, Suarez M, Barrio A, et al. (1999) Synthesis and Antiprotozoan Evaluation of New 3, 5-disubstituted-tetrahydro-1, 3, 5-thiadiazinan-2-thione derivatives. Arzneimittelforschung 49(9): 764-769.

17. Coro J, Pérez R, Rodríguez H, Suárez M, Vega C, et al. (2005) Synthesis and antiprotozoan evaluation of new alkyl-linked bis 2-thioxo-[1, 3, 5] thiadiazinan-3-yl carboxylic acids. Bioorganic medicinal chemistry 13(10): 3413-3421.

18. Rodríguez H, Coro J, Suárez M, Martínez Álvarez R, Martín N, et al. (2012) Liquid phase organic synthesis of 3, 5-disubstituted 1, 3, 5-thia-diazinane-2-thione derivatives on polyethylene glycol PEG support. Arkivoc 8: 326-338.

19. Coro J, Alvarez Puebla R, Montero AL, Suárez M, Martin N, et al. (2008) A computational approach to the synthesis of 1, 3, 5-thiadiazinane-2-thiones in aqueous medium theoretical evidence for water promoted heterocyclization. Journal of molecular modeling 14(7): 641-647.

20. Arshad N, Hashim J, Minhas MA, Aslam J, Ashraf T, et al. (2018) New series of 3, 5-disubstituted tetrahydro-2H-1, 3, 5-thiadiazine thione THTT derivatives synthesis and potent antileishmanial activity. Bioorganic Medicinal Chemistry Letters 28(19): 3251-3254.

21. Hussein MA, El Shorbagi AN, Khallil AR (2001) Synthesis and antifungal activity of 3, 3'-ethylenebis 5-alkyl-1, 3, 5-thiadiazine-2-thiones. Archiv der Pharmazie 334(10): 305-308.

22. Tetteh S, Dodoo D, Appiah Opong K, Tuffour R (2014) Spectroscopic characterization in vitro Cytotoxicity, and Antioxidant Activity of Mixed Ligand Palladium II Chloride Complexes Bearing Nucleobases. J Inorg Chem 8: 675-688.